Title	Disorder influenced absorption line shapes of a chromophore coupled to two-level systems
Author(s)	Shenai, Prathamesh M.; Chernyak, Vladimir; Zhao, Yang
Citation	Shenai, P. M., Chernyak, V., & Zhao, Y. (2013). Disorder Influenced Absorption Line Shapes of a Chromophore Coupled to Two-Level Systems. Journal of Physical Chemistry A, 117(47), 12320–12331.
Date	2013
URL	http://hdl.handle.net/10220/19722
Rights	© 2013 American Chemical Society. This is the author created version of a work that has been peer reviewed and accepted for publication by Journal of Physical Chemistry A, American Chemical Society. It incorporates referee's comments but changes resulting from the publishing process, such as copyediting, structural formatting, may not be reflected in this document. The published version is available at: http://dx.doi.org/10.1021/jp4080042.

THE JOURNAL OF PHYSICAL CHEMISTRY A

Article

pubs.acs.org/JPCA

Disorder Influenced Absorption Line Shapes of a Chromophore Coupled to Two-Level Systems

Prathamesh M. Shenai,[†] Vladimir Chernyak,[†,‡] and Yang Zhao*[,†]

[†]Division of Materials Science, Nanyang Technological University, Singapore 639798

[‡]Department of Chemistry, Wayne State University, Detroit, Michigan 48202, United States

ABSTRACT: We have carried out a theoretical and numerical study of disorder-induced changes in the absorption line shape of a chromophore embedded in a host matrix. The stochastic sudden jump model is employed wherein the host matrix molecules are treated as noninteracting two-level systems (TLSs) occupying points on a three-dimensional lattice with randomly oriented dipole moments. By systematically controlling the degree of positional disorder (α) attributed to them, a perfectly crystalline ($\alpha = 0$) or glassy environment ($\alpha = 1$) or a combination of the two is obtained. The interaction between the chromophore and TLSs is assumed to be of the dipole−dipole form. With an increase in α, the broadening of the absorption line shape was found to follow a power-law behavior. More importantly, it is revealed in the long-time limit that the resultant line shape is Gaussian in the absence of disorder but transforms to Lorentzian for a completely disordered environment. For an arbitrarily intermediate value of α, the resultant line shape can be approximately fitted by a linear combination of Gaussian and Lorentzian components. The Lorentzian profile for the disordered medium is attributed to the chomophore−TLS pairs with vanishingly small separation between them.

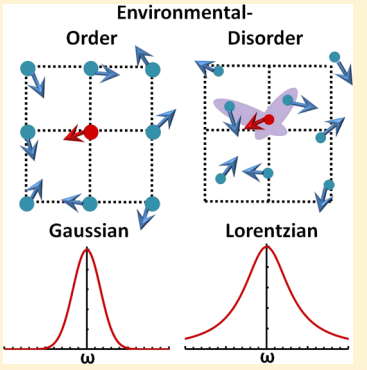

I. INTRODUCTION

The advent of single molecule spectroscopy (SMS) in recent decades has proved to be of immense importance in gaining vital information about submicroscopic structure, dynamics, and intermolecular interactions via optical probing of single molecules, atoms, or ions embedded in condensed matter systems.[1,2] The richness of information derived from SMS can be ascribed to the fact that the measurements it yields are based not on ensemble averages as in traditional spectroscopic techniques, but instead on the distributions of spectral dynamical behavior of a number of individual molecules. SMS experiments generally involve time-domain measurements such as spectral diffusion kernels or frequency-domain measurements such as absorption line shapes.[3−6] The electronic energy levels of a chromophore being sensitive to its environment, the fluctuations in the surrounding molecules and their interactions with the chromophore influence the chromophore's absorption frequency. Typically such modulations lead to line shape broadening, the characteristics of which directly reflect the host−guest interactions. In particular, the application of SMS to measure absorption spectra of individual chromophores in disordered media such as glasses has revealed a remarkably wide range of behavior including the movement of spectral peaks in successive measurements, known as spectral diffusion,[7−9] and strong variations in the observed line shapes and line widths.[10] Generally, the absorption spectrum of a chromophore dispersed at a low concentration in structurally disordered hosts, such as liquids or glasses, is inhomogeneously broadened.[11−14] Such inhomogeneous broadening reflects the extent of the microscopic disorder around the chromophore, the transition frequency of which can be taken to arise from a superposition of contributions from crystal defects in the case of amorphous media or described by a sum of pairwise interactions with each solvent molecule in the case of liquid media. It thus becomes amply clear that SMS in such systems, especially at very low temperatures, can play an important role in elucidating the structure and dynamics of glasses, which itself has been a perplexing research field.

Glasses are amorphous solids characterized by the structural disorder that gives rise to their many intriguing properties such as the anomalous behavior of acoustic and thermal properties at very low temperatures.[15] A celebrated phenomenological model based on the so-called two-level systems (TLSs) proposed independently by Anderson et al.[16] and Phillips[17] has proved to be greatly successful in explaining many of such anomalous characteristics of amorphous materials.[18−26] Within this model, the disorder in amorphous materials is assumed to be characterized by the presence of randomly scattered defects in which an atom or a group of atoms can occupy one of the two minima on the potential energy surface. Each TLS can be represented as a particle in an asymmetric double-well potential energy surface with respect to some generalized configurational coordinate as shown schematically in Figure 1. It can thus be fully specified with two parameters A and M, which are the energy asymmetry between the left ($|L\rangle$) and right ($|R\rangle$) well

Received: August 9, 2013
Revised: October 24, 2013

   dx.doi.org/10.1021/jp4080042 | J. Phys. Chem. A XXXX, XXX, XXX−XXX

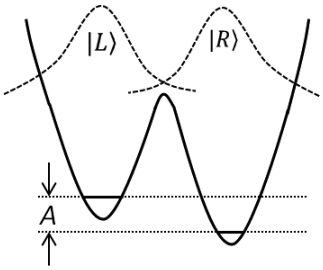

Figure 1. Asymmetric double-well potential shown along with the two states localized in the left well (|L⟩) and right well (|R⟩).

states and the tunneling matrix element between them, respectively. The transition or flipping between the two states is believed to take place via quantum-mechanical tunneling, and thus TLSs are also referred to as tunneling TLSs.[15,27] The exceptional success of the TLS model, however, belies an equally surprising inadequacy in the fundamental understanding of their microscopic nature and origin, despite great research efforts.[28,29] Encouragingly, some studies have indicated possible interpretation of the TLSs as the motion of domain walls[30] while others have proposed SMS-based experiments as the test bed for the validity of the standard TLS model.[31]

To obtain insights into the structure and dynamics of glassy materials and their interactions with embedded optical probes, a number of analytical and numerical studies have been undertaken. The stochastic sudden jump model pioneered by Klauder and Anderson[32] in the context of magnetic resonance experiments was adapted successfully by a number of studies to examine the spectral properties of single chromophores in glasses.[33−43] Suarez and Silbey proposed a microscopic Hamiltonian for a generalized spin-boson model to study the dynamics of TLSs and demonstrated its correlation with the stochastic sudden jump model.[39] The fluctuations in the transition energies of a chromophore surrounded by TLSs were studied with the help of a random walk theory by Zumofen and Klafter.[40] Under the assumption of dipolar−dipolar interactions between the chromophore and randomly distributed defects surrounding it, Orth et al.[41] found the defect density to be an important parameter. While at the smallest and largest values of defect density the absorption line shape was found to be of Lorentzian and approximately Gaussian forms, respectively, for the intermediate values the line shapes were found to be approximated well by a sum of Gaussian curves. Geva et al. calculated the distribution of SMS line widths and estimated the TLS−chromophore coupling constant by using it as the sole parameter fit to the experimental data for terrylene in polystyrene[42] as well as similar other systems.[43] In nearly all these studies, the interactions between the environmental TLSs themselves are typically disregarded. Brown and Silbey validated this assumption by demonstrating that the influence of explicit inclusion of TLS−TLS coupling on the line width distributions is insignificant.[44] More recently, Naumov et al. calculated the first four moments of spectral line profiles for single molecules in organic glasses, through which they were able to estimate important coupling parameters as well as the minimum chromophore−TLS separation distance.[45] In a recent work, Wu and Zhao extended the traditional spin-boson model to study the properties of a TLS interacting with a boson bath as well as an additional spin bath.[46] The finite coupling between the TLS and the spin bath was found to assist the steady-state flipping of the TLS.

In this paper, we investigate the spectral line shape of chromophores that are sufficiently dilute so that they do not interact with each other. We employ a model in which a chromophore is coupled to a collection of noninteracting flipping TLSs and calculate the frequency-domain absorption line shape, with an emphasis on studying the effects of spatial and steric disorder of TLSs, which have not been evaluated systematically in the existing literature. For simulating crystalline media the TLSs reside on fixed lattice points, while for the glassy surroundings spatial disorder is introduced to the TLSs. The final absorption line shape is obtained as an average over an initial distribution of static TLS configurations. By modeling all the host TLSs to be identical, we can extract the influence of disorder in the TLS distribution on the chromophore's absorption line shape, which is obscured within the standard tunneling TLS model due to the distribution of TLS parameters. Given the as-yet lack of clarity on the physical form of the idealized TLSs, the present study of spectral features of chromophores may yield important insights in understanding the submicroscopic distribution of surrounding TLSs. This paper is organized as follows. The theoretical model and computational details are outlined in section II. The results are presented and discussed in detail in section III, and the conclusions are drawn in section IV.

II. THEORY AND COMPUTATIONAL MODEL

In this work, we examine the characteristics of the absorption line shape of a chromophore embedded in a solid matrix. The chromophore, which can be considered as an optical impurity or a probe molecule, is thus modeled as an electronic TLS with its ground (|g⟩) and excited (|e⟩) states separated by energy equal to $\hbar\omega_{eg}$. The environment, generally disordered media like glasses, to which this chromophore is coupled, is modeled as a collection of TLSs.[35,38,42,44] These TLSs in the host matrix are generally considered to correspond to the asymmetric double-well potential as a function of a generalized configurational coordinate. The energy asymmetry between the two localized zero-order states for the jth TLS is A_j, and the tunneling matrix element is M_j. Within this standard model, the absorption frequency of the chromophore is thought to depend upon the instantaneous states of the surrounding TLSs.[44] Thus we can introduce a time-dependent stochastic occupation variable ξ_j which is set to 0 (1) if the jth TLS is in its ground (excited) state. With the stochastic sudden jump model, which is among the most popular models employed to study the absorption line shape of a chromophore embedded in glassy systems,[32,33,39,44] we can write the renormalized transition frequency of the chromophore as

$$\omega_{eg} = \omega_{eg}^{0} + \sum_{j} \upsilon_j \xi_j \qquad (1)$$

where ω_{eg}^{0} is the transition frequency of the chromophore when all the TLSs are in the ground state and υ_j is the perturbation that the jth TLS in its excited state induces to the chromophore transition frequency. Being a stochastic variable, the statistical properties of ξ_j are determined by the net relaxation rate $K_j = k_j^{u} + k_j^{d}$, where k_j^{u} (k_j^{d}) is the upward (downward) transition rate. At low temperature, as the relaxation mechanism in host TLSs is assumed to be dominated by phonon-assisted tunneling, we can write[44]

dx.doi.org/10.1021/jp4080042 | J. Phys. Chem. A XXXX, XXX, XXX−XXX

$$k_j^{u} = C\epsilon_j M_j^{2} \frac{\exp(-\epsilon_j/k_B T)}{1 - \exp(-\epsilon_j/k_B T)} \quad (2a)$$

$$k_j^{d} = C\epsilon_j M_j^{2} \frac{1}{1 - \exp(-\epsilon_j/k_B T)} \quad (2b)$$

where C is the TLS−phonon coupling constant, T is temperature, and $\epsilon_j = (A_j^2 + M_j^2)^{1/2}$ is the energy splitting of the eigenstates of the jth TLS. Furthermore, in thermal equilibrium, the probability (P_j^k) of finding the jth TLS in state k (k = 0,1) is given as

$$P_j^k = p_j \delta_{k,1} + (1 - p_j)\delta_{k,0} \quad (3)$$

where $p_j = [\exp(\epsilon_j/k_B T) + 1]^{-1}$ is the probability for the jth TLS being in the excited state, and k_B is the Boltzmann constant.

The TLSs causing the fluctuations in the chomophore's absorption frequency are themselves considered to be non-interacting as such TLS−TLS coupling has been shown to exert negligible influence on the spectral properties of the chromophore.[44] We adopt the approach proposed by Reilly and Skinner, and for the chromophore embedded in a sea of uncorrelated and identical TLSs, the time-domain response function $J(t)$ can be obtained as a product of individual response functions $J_j(t)$:[35,38]

$$J(t) = \exp(-i\omega_{eg} t) \prod_j J_j(t) \quad (4)$$

where

$$J_j(t) = \exp\left(\frac{-b_j t}{2}\right)\left[\cosh(\Lambda_j t) + \frac{2d_j - b_j}{2\Lambda_j}\sinh(\Lambda_j t)\right] \quad (5)$$

with

$$\Lambda_j = \sqrt{\frac{K_j^2}{4} - \frac{v_j^2}{4} - i\left(p_j - \frac{1}{2}\right)v_j K_j} \quad (6a)$$

$$b_j = iv_j + K_j \quad (6b)$$

$$d_j = K_j + iv_j(1 - p_j) \quad (6c)$$

The linear absorption line-shape function $I(\omega)$ obtained via Fourier transformation of $J(t)$ is then written as

$$I(\omega) = \frac{1}{\pi}\mathrm{Re}\int_0^\infty dt\, e^{i\omega t} J(t) \quad (7)$$

The interaction between the chromophore and a TLS is clearly an important consideration, and in this work we adopt the commonly employed assumption of its dipole−dipole nature. One thus obtains

$$v_j = \frac{Bf_j}{r_j^3} = \frac{B(\boldsymbol{n}_j \cdot \boldsymbol{n} - 3(\boldsymbol{n}_j \cdot \hat{\boldsymbol{r}}_j)(\boldsymbol{n} \cdot \hat{\boldsymbol{r}}_j))}{r_j^3} \quad (8)$$

where f_j is a dimensionless angular factor associated with the interaction between the chromophore and the jth TLS, whose positions (dipole directions) are $\boldsymbol{r}$ and $\boldsymbol{r}_j$ ($\boldsymbol{n}$ and $\boldsymbol{n}_j$), respectively; $r_j = |\boldsymbol{r}_j - \boldsymbol{r}|$ and $\hat{\mathbf{r}}_j = (\boldsymbol{r}_j - \boldsymbol{r})/r$ are the distance and the direction between them, respectively, and $B = A_j C'/\epsilon_j$ with C' as the TLS−chromophore coupling constant. This approximation originates from the early studies of disordered systems in which it was found that various experimental results could be corroborated well by theoretical considerations under the assumption of dipolar TLS−TLS interactions.[32,47−49] The exact correspondence of the dipoles corresponding to TLSs with a physical meaning is not entirely clear considering the ambiguities in the nature of the TLSs themselves. It is, however, well-known that a local perturbation due to state transitions of a TLS gives rise to a strain field that shows r^{-3} dependence characteristic to dipolar type.[19,43,50−52] Accordingly, the nonresonant chromophore−TLS interactions of dipolar nature, owing to the effective "elastic dipole moment" of a TLS, were also found to agree well with spectroscopic results.[53] In their derivation of the stochastic model from the microscopic Hamiltonian, Suarez and Silbey argued that the chromophore and the TLSs can be considered to be both coupled to the same set of phonons, acting as a boson field.[39] It thus mediates an elastic dipole−dipole interaction between them that consequently leads to the spectral diffusion of the chromophore. Furthermore, by doping nanocrystals containing rare-earth ions as optical impurities in amorphous matrixes, Meltzer et al. have recently proposed to have obtained encouraging evidence for long-range dipole−dipole interactions between the probe and the TLSs.[54]

Finally, we present the details of the numerical approach for our lattice-based simulations. The simulation volume is divided into $N'^3(N' \times N' \times N')$ cubic unit cells each of a side length of a_0. The central unit cell consists of the sole chromophore, while the remaining unit cells contain a total of $N = (N'^3 - 1)$ host TLSs on a single-occupancy basis. For the chromophore as well as the other TLSs, the dipoles are randomly oriented such that $-1 \le \cos\theta < 1$ and $-\pi \le \phi < \pi$, where θ as the azimuthal angle in the xy plane and ϕ as the polar angle are defined in the standard way from the x and z axes, respectively. As shown in Figure 2, the precise position of the chromophore or a TLS is

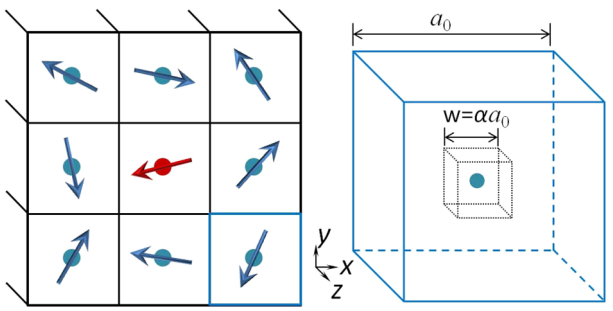

Figure 2. (left) Schematic cross section in the xy plane of the simple cubic lattice structure in which each of the unit cells of length a_0 is occupied by a TLS (blue dot) except for the central unit cell, which is occupied by the chromophore (red dot). The corresponding dipole moments (arrows) are randomly oriented. (right) Magnified view of a unit cell (solid blue border) showing the position of its occupant TLS ascribed randomly within a smaller cubic subunit of length $w = \alpha a_0$.

assigned to a randomly selected point inside an even smaller cubic subunit of sides of length $w = \alpha a_0$, with α as the parameter to control the degree of spatial disorder. Clearly, for the perfectly ordered case $\alpha = 0$, all the TLSs and the chromophore occupy points on the simple cubic lattice. With an increase in $\alpha = 0$, the perturbation to the positions about the lattice points increases. Thus, $\alpha = 1$ corresponds to a completely random distribution of TLSs, thereby simulating a glassy environment. By varying α from 0 to 1, we can thus

dx.doi.org/10.1021/jp4080042 | J. Phys. Chem. A XXXX, XXX, XXX−XXX

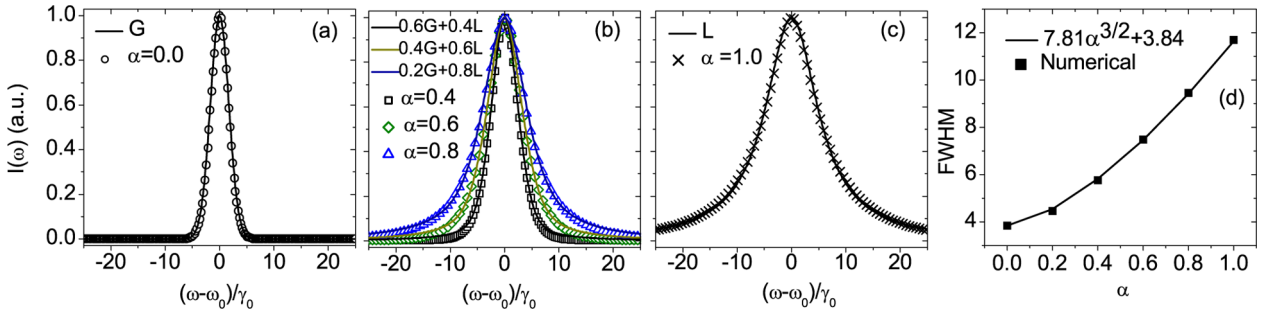

Figure 3. Calculated absorption line shapes for (a) $\alpha = 0.0$ (hollow circles); (b) $\alpha = 0.4$ (hollow squares, black), 0.6 (hollow diamonds, green), and 0.8 (hollow triangles, blue); and (c) $\alpha = 1.0$ (crosses). The corresponding fitting with the Gaussian curve (G) in (a), Lorentzian (L) in (c), and their linear combinations $[\alpha L + (1 - \alpha)G]$ in (b) are shown as unbroken curves. (d) fwhm of the absorption peaks as a function of α.

control the degree of disorder in the system, which may correspond to the increasingly amorphous nature of the chromophore's environment. Most of our numerical simulations are based on $N' = 11$, which has been verified to yield converged results. Further, in our calculations, we set the parameters $C = 3.9 \times 10^8$ K^{-3} s^{-1}, $C' = 3.75 \times 10^{11}$ nm^3 s^{-1}, $M_j = 0.008$ K, $A_j = 0.006$ K, $a_0 = 4.43$ nm, and $T = 1.7$ K, which are representative of typical glassy systems.[42,44,55] In numerical results, frequencies are scaled by a factor of $\gamma_0 = B/a_0^3 = 2.588$ GHz, which carries a meaning of typical dipole coupling, i.e., the value of dipole coupling at an average chromophore−TLS distance of a_0. The total simulation time is set to 20 ns, and results are averaged over 30 000 randomly sampled iterations.

III. ABSORPTION LINE SHAPES

A. Effect of Disorder. The numerical results on calculated absorption line shapes for $\alpha = 0.0$, 0.4, 0.6, 0.8, and 1.0, as well as their fitting by either Gaussian (G) or Lorentzian (L) functions or their linear combinations $[\alpha L + (1 - \alpha)G]$, are shown in Figure 3. The absorption spectra shown here are all normalized by the peak intensity. For $\alpha = 0.0$, which refers to the ordered distribution of TLSs and the chromophore on cubic lattice, Figure 3a shows that the obtained line shape is fitted well by a Gaussian profile, in agreement with previous results.[40,41] We further note that this case amounts to the steric disorder, as the dipole moments of the TLSs are randomly oriented but their positions are fixed. Thus an ensemble average over the distribution of dipole directions implies that the chromophore−TLS interactions along different directions will be different. This may result in the inhomogeneously broadened Gaussian profile, which is consistent with earlier results showing the broadening due to the static heterogeneity to be inhomogeneous.[37] On the other hand, for $\alpha = 1.0$, which represents the glassy or completely disordered environment, it is evident from Figure 3c that the line shape is fitted well by a Lorentzian curve. In this case the positions as well as dipole directions of the TLSs are completely disordered within their residence cells. Therefore, an ensemble average with sufficient configurational sampling should imply nearly isotropic distribution of the TLSs around the chromophore. The Lorentzian line shape obtained for this case then results from the homogeneous broadening.

For the intermediate regime an increase in α can be observed to change the line shape as well as increase its full width at half-maximum (fwhm), as shown in Figure 3b. As the finite fwhm results from the chromophore−TLS interactions, it is apparent that the stronger the interaction, which in turn depends on the distance between them, the greater its influence on the broadening. An increase in α from 0 will decrease the average chromophore−TLS separation due to increased positional perturbations and thus increase the resulting fwhm. Furthermore, such a gradual increase in the degree of spatial disorder with an increase in α implies a gradual change from an inhomogeneous to a homogeneous influence of the environment. Accordingly, the absorption line shape can be observed to be approximately fitted by a superposition of the individual G and L components, $[\alpha L + (1.0 - \alpha)G]$. The calculated fwhm exhibits a power-law dependence on α as shown in Figure 3d. In essence, the numerical results demonstrate a smooth transition of the line shape from Gaussian to Lorentzian with an increase in spatial disorder of the host matrix TLSs.

B. Ordered Environment: Gaussian Line Shape. In this subsection, we present the analytical study to probe the conditions under which the absorption line shape is of the Gaussian form. We first note that the parameters used in our numerical simulations correspond to the high-temperature and static regime. Thus, we can set $p_j = 0.5$ and $K_j = 0$ in eqs 5, 6a, 6b, and 6c, which results in

$$J_j(t) = \frac{1}{2}(1 + e^{-i\upsilon_j t}) \tag{9}$$

in full accordance with the well-known expression for the static limit.[35,38] We reiterate that the static limit expression given by eq 9 can be obtained immediately by assuming that a TLS does not have time to flip even once, so that it simply reflects the averaging over initial conditions with the probability 1/2 to be in either of the states, which corresponds to the high-temperature limit. The time-domain response function averaged over positional disorder (the chromophore and the TLSs distributed within their residence cells) and the dipole directions is denoted by $\overline{J}(t)$, and can be represented in a form

$$\overline{J}(t) = \int d\boldsymbol{r}\, \rho(\boldsymbol{r}) \int d\boldsymbol{n} \prod_j \overline{J}_j(t; \boldsymbol{r}, \boldsymbol{n}) = \int d\boldsymbol{r}\, \rho(\boldsymbol{r}) \int d\boldsymbol{n}\, \overline{J}(t; \boldsymbol{r}, \boldsymbol{n}) \tag{10}$$

$$\overline{J}_j(t; \boldsymbol{r}, \boldsymbol{n}) = \int d\boldsymbol{r}_j\, \rho_j(\boldsymbol{r}_j) \int d\boldsymbol{n}_j \frac{1}{2}[1 + \exp(-i\upsilon_j t)] \tag{11}$$

where $\rho(\boldsymbol{r})$ and $\rho(\boldsymbol{r}_j)$ are the distribution functions of the chromophore and TLSs positions, respectively, with homogeneous distributions over the dipole directions, as assumed in our numerical simulations. The integration measures in eqs 10 and 11 are normalized

dx.doi.org/10.1021/jp4080042 | J. Phys. Chem. A XXXX, XXX, XXX−XXX

$$\int d\boldsymbol{n} = \int d\boldsymbol{n}_j = \int d\boldsymbol{r}_j\, \rho(\boldsymbol{r}_j) = \int d\boldsymbol{r}\, \rho(\boldsymbol{r}) = 1 \tag{12}$$

If the distance between a TLS and the chromophore is large enough so that the value v_j of the coupling is small compared to the absorption line width, i.e., $v_j t \ll 1$ for relevant values of t, we can expand the exponent in eq 11 up to second order in $v_j t$ to capture the corrections to the real part as well as the imaginary part. Further performing the integration over $\boldsymbol{n}_j$ explicitly, we obtain within the chosen accuracy

$$\bar{J}_j(t;\, \boldsymbol{r},\, \boldsymbol{n}) = 1 - g_j(t;\, \boldsymbol{r},\, \boldsymbol{n}) = \exp(-g_j(t;\, \boldsymbol{r},\, \boldsymbol{n})) \tag{13}$$

with

$$g_j(t;\, \boldsymbol{r},\, \boldsymbol{n}) = -\sigma_j(\boldsymbol{r},\, \boldsymbol{n})\frac{t^2}{2} \tag{14}$$

where

$$\sigma_j(\boldsymbol{r},\, \boldsymbol{n}) = \frac{1}{2}\int d\boldsymbol{r}_j\, \rho_j(\boldsymbol{r}_j) \int d\boldsymbol{n}_j\, v_j^2 \tag{15}$$

Note that the linear in time t term in eq 14 vanishes as a result of integration of the angular factor f_j from eq 8 over $\boldsymbol{n}_j$. Substituting eq 8 into eq 15 and performing integration over $\boldsymbol{n}_j$, we arrive at

$$\sigma_j(\boldsymbol{r},\, \boldsymbol{n}) = \sum_{ab=1}^{3} \alpha_j^{ab}(\boldsymbol{r}) n^a n^b \tag{16}$$

where a and b label the Cartesian coordinates, with

$$\alpha_j^{ab}(\boldsymbol{r}) = B^2 \int d\boldsymbol{r}_j\, \rho_j(\boldsymbol{r}_j) \frac{\delta^{ab} + 3\hat{r}_j^a \hat{r}_j^b}{6\,|\boldsymbol{r}_j - \boldsymbol{r}|^6} \tag{17}$$

and we reiterate that $\hat{\boldsymbol{r}}_j$ is the unit vector in the direction of $(\boldsymbol{r}_j - \boldsymbol{r})$.

If the approximation made to derive eq 13 is valid for all TLSs, we have

$$\bar{J}(t;\, \boldsymbol{r},\, \boldsymbol{n}) = \exp\left(-\frac{t^2}{2}\sum_{ab} \alpha^{ab}(\boldsymbol{r}) n^a n^b\right) \tag{18}$$

with

$$\alpha^{ab}(\boldsymbol{r}) = \sum_j \alpha_j^{ab}(\boldsymbol{r}) \tag{19}$$

which means that, under the above assumption and if the position and dipole direction of the chromophore is fixed, even in the presence of disorder in the positions and dipole orientations of the TLSs, the absorption line has a Gaussian shape. Disorder in the chromophore positions, as well as random distribution of its dipole orientation, will create deviations from the Gaussian shape.

There still exists a situation in which the random distribution of the chromophore's dipole orientation does not lead to deviations of the absorption line from its Gaussian shape, namely, when the chromophore is fixed at the center of its cell $\boldsymbol{r} = 0$, which can be equivalently written as $\rho(\boldsymbol{r}) = \delta(\boldsymbol{r})$, whereas the distribution functions that describe disorder in the TLSs' positions preserves the symmetry of the cubic lattice. Note that the disorder considered in this paper obviously satisfies the above property. In this case we deal with $\alpha^{ab}(0)$ [defined for the general case by eq 19] that can be viewed as a symmetric rank 2 tensor, invariant under the rotations that preserve the cubic lattice. A tensor that satisfies the above property is known to be, up to a scalar multiplicative factor, the Kronecker delta δ^{ab}, which implies

$$\alpha^{ab}(0) = \frac{1}{3}\,\mathrm{Tr}(\alpha(0))\delta^{ab} \tag{20}$$

Taking the trace in eq 17, and making use of eqs 19 and 20, we obtain

$$\bar{J}(t;\, 0,\, \boldsymbol{n}) = \exp\left(-\frac{\sigma t^2}{2}\right) \tag{21}$$

with

$$\sigma = \sum_j \int d\boldsymbol{r}_j\, \rho_j(\boldsymbol{r}_j) \frac{B^2}{3\,|\boldsymbol{r}_j|^6} \tag{22}$$

which reproduces the Gaussian absorption line shape that is independent of the chromophore's dipole orientation $\boldsymbol{n}$, and therefore the line shape does not undergo any change upon any averaging over the latter.

For comparison between the analytical predictions and the numerical results, we have further applied eq 22 to evaluate σ for the model used in numerical simulations with $\alpha = 0$. For this case, the pairwise distances between the chromophore and the TLSs take up discrete values and we obtain $\sigma/\gamma_0^2 = 2.92$. From Figure 4, it can be seen that with this value of σ, the averaged response function $\bar{J}(t)$ from eq 21 yields a quite satisfactory fit to the numerical results.The above quantitative arguments thus perfectly rationalize the Gaussian line shape not only in the absence of disorder and averaging over all dipole orientations, but also for a special type of disorder when the positions of the chromophore together with its nearest neighbor TLSs are fixed at the centers of their residence cells.

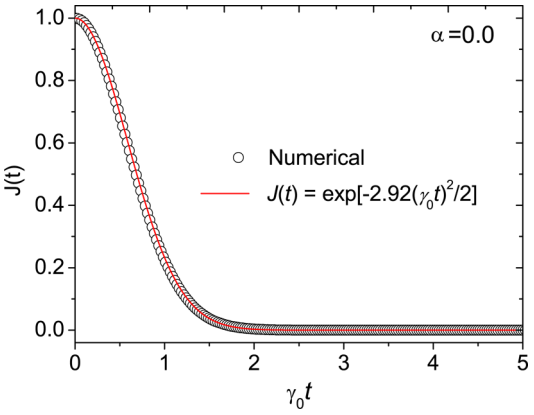

Figure 4. For perfectly crystalline TLS environment (α = 0.0), the averaged response function calculated from numerical simulations (hollow circles) and its comparison with the analytical expressions of eqs 21 and 22

Equation 22 implies that the contribution to the response function is dependent mainly on the TLSs that are located relatively closer to the chromophore and thus effectively on the distribution of chromophore−TLS pairwise distances, especially for $|r_j| \leq a_0$. While the minimum average separation is equal to a_0 when $\alpha = 0$, it gradually decreases with an increase in α and can even be vanishingly small for $\alpha = 1$. The presence of TLSs in such close proximity of the chromophore implies a much stronger perturbation to the transition frequency of the

dx.doi.org/10.1021/jp4080042 | J. Phys. Chem. A XXXX, XXX, XXX−XXX

chromophore compared to that due to the relatively distant TLSs. To study the role of local order in the distribution of TLSs, we carry out simulations with additional constraints by which the chromophore and its six nearest neighbors are fixed to the corresponding lattice points as shown in Figure 5a. The

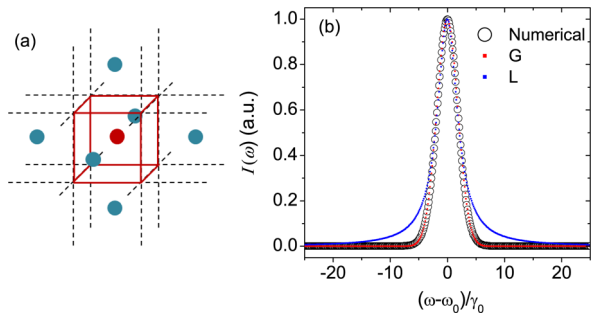

Figure 5. (a) Schematic of the model with the chromophore and its six nearest neighbor TLSs fixed at the centers of their unit cells. (b) Resulting absorption line shape and its fitting by Gaussian (G) and Lorentzian (L) functions when $\alpha = 1.0$ for the remaining TLSs.

dipole moments of the spatially fixed TLSs and the chromophore are, however, still allowed to be randomly oriented. The rest of the TLSs are subjected to the regular condition of $\alpha = 1$. Under these constraints which provide some degree of local order, the minimum chromophore−TLS separation is $(a_0/\sqrt{2})$ and corresponds to the case of a TLS from a unit cell that shares an edge with the unit cell of the chromophore being positioned midway along that edge. Despite completely disordered distant−TLSs, the resulting absorption line shape depicted in Figure 5b is found to be well fitted by a Gaussian function. This observation points out that the morphing of the line shape from Gaussian to Lorentzian profile when α is changed from 0 to 1 can be ascribed to the strong effect exerted by the TLSs in the immediate vicinity of the chromophore. Further support for this important distance dependence can be found in Figure 6a, which shows the

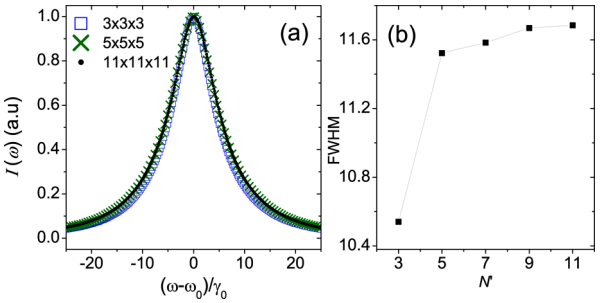

Figure 6. For $\alpha = 1.0$, (a) absorption line shapes for different lattice sizes with $N' = 3$ (hollow blue squares), 5 (green crosses), and 11 (black dots), and (b) corresponding fwhm for increasing N'.

calculated absorption line shapes from the regular (unconstrained) simulations with $\alpha = 1.0$ for various lattice sizes. $N' = 3$ is the smallest possible lattice-based arrangement of TLSs around a chromophore, and yet, barring a small difference in fwhm, the Lorentzian line shape it yields is nearly identical to that obtained with larger lattices. Figure 5b shows the convergence achieved for the fwhm as a function of N'. This further emphasizes that, even for the largest lattice size studied in this work, the predominant contribution to the spectral line shape is provided by the close TLS neighbors of the chromophore, an observation that has important bearing in the study of Lorentzian line shapes for $\alpha = 1$ presented in subsection C.

C. Disordered Environment: Lorentzian Line Shape.

The qualitative analysis, as well as the quantitative arguments, in subsection B, clearly demonstrates that a substantial deviation of the absorption line from its Gaussian shape in the case of complete or almost complete disorder originates from the configurations when a TLS comes very close to the chromophore. This renders invalid the approximation invoked to derive eq 13. To rationalize the Lorentzian line shape in this case, we need to adapt our approach and evaluate the integral over $\boldsymbol{n}_j$ in eq 11 exactly without making any expansion. To that end we fix $\boldsymbol{r}$ and $\boldsymbol{n}$, denote $r_j = |\boldsymbol{r}_j - \boldsymbol{r}|$, and represent v in a form

$$v(\boldsymbol{r}_j, \boldsymbol{n}_j) = \frac{B}{r_j^3}(\boldsymbol{n} - 3(\boldsymbol{n}\cdot\hat{\boldsymbol{r}}_j)\hat{\boldsymbol{r}}_j)\cdot\boldsymbol{n}_j \tag{23}$$

We then compute

$$|\boldsymbol{n} - 3(\boldsymbol{n}\cdot\hat{\boldsymbol{r}}_j)\hat{\boldsymbol{r}}_j| = \sqrt{1 + 3(\boldsymbol{n}\cdot\hat{\boldsymbol{r}}_j)^2} \tag{24}$$

so that

$$\int \mathrm{d}\boldsymbol{n}_j\, \mathrm{e}^{-\mathrm{i}v t} = \frac{1}{4\pi} 2\pi \int_0^\theta \sin\theta\, \mathrm{d}\theta \times \exp\left(\mathrm{i}\frac{Bt}{r_j^3}\sqrt{1 + 3(\boldsymbol{n}\cdot\hat{\boldsymbol{r}}_j)^2}\,\cos\theta\right) = \frac{\sin(\Omega(\boldsymbol{r}_j)t)}{\Omega(\boldsymbol{r}_j)t} \tag{25}$$

where we have introduced

$$\Omega(\boldsymbol{r}_j) = \frac{B\sqrt{1 + 3(\boldsymbol{n}\cdot\hat{\boldsymbol{r}}_j)^2}}{r_j^3} \tag{26}$$

Substituting eq 25 into eq 11, we arrive at

$$\bar{J}_j(t; \boldsymbol{r}, \boldsymbol{n}) = 1 - p_j \int \mathrm{d}\boldsymbol{r}_j\, \rho_j(\boldsymbol{r}_j)\, h(\boldsymbol{r}_j, t) \tag{27}$$

where we have introduced

$$h(\boldsymbol{r}_j, t) = 1 - \frac{\sin(\Omega(\boldsymbol{r}_j)t)}{\Omega(\boldsymbol{r}_j)t} \tag{28}$$

Here, we keep the arbitrary value of the probability p_j for a TLS to be in the excited state, rather than setting it to 1/2. Note that the function $h(\boldsymbol{r}_j t)$ is continuous (although not smooth) at $\boldsymbol{r}_j = 0$, and $h(\boldsymbol{r}_j, t) \sim r_j^{-6}$ for large values of r_j.

To rationalize the Lorentzian line shape in the $\alpha = 1$ case of complete disorder, we start with considering a similar, still in the least not less physical, model of disorder when the chromophore position is fixed, whereas N identical TLSs are independently and randomly distributed inside some region $\mathcal{U} \subset \mathbb{R}^3$ of large enough size with the volume V. Formally this means that

$$\rho_j(\boldsymbol{r}_j) = V^{-1}, \quad \boldsymbol{r}_j \in \mathcal{U}, \quad j = 1, \ldots, N \tag{29}$$

Substituting eq 29 into eq 27, we can make use of the $\sim r_j^{-6}$ behavior of h at large values of r_j, as well as the assumption of large size of $\mathcal{U}$ and extend integration in eq 27 from $\mathcal{U} \subset \mathbb{R}^3$ to the entire Euclidean space R^3, followed by switching to the variables $\boldsymbol{r}_j = (x, \hat{\mathbf{r}}_j)$ with $x = (\Omega t)^{-1}$, which results in

dx.doi.org/10.1021/jp4080042 | J. Phys. Chem. A XXXX, XXX, XXX−XXX

$$\overline{J}_j(t) = 1 - p_j \frac{\zeta B}{V} t \approx \mathrm{e}^{-\zeta p_j B V^{-1} t} \tag{30}$$

with the dimensionless factor

$$\zeta = \frac{4\pi}{3} \int_0^1 \mathrm{d}\tau \sqrt{1 + 3\tau^2} \int_0^\infty \mathrm{d}x \left(1 - x \sin \frac{1}{x}\right) = \frac{\pi^2}{3} \int_0^1 \mathrm{d}\tau \sqrt{1 + 3\tau^2} \tag{31}$$

Finally, we arrive at an expression that immediately leads to the Lorentzian absorption line shape:

$$\overline{J}(t) = (\overline{J}_j(t))^N = \mathrm{e}^{-\gamma t}, \qquad \gamma = \xi p_j B n \tag{32}$$

where $n = N/V$ is the TLS concentration and ζ is a dimensionless factor of the order of 1 that reflects a particular model of disorder.

We are now in a position to consider the model of disorder that has been used in our numerical simulations. We start with noting that the exponential shape $\overline{J}(t) = \mathrm{e}^{-\gamma t}$ of the time response function [e.g., as in eq 32] is equivalent to the Lorentzian shape

$$I(\omega) = \frac{\gamma}{\omega^2 + \gamma^2} \tag{33}$$

where, to simplify the formulas, we set $\omega_{\mathrm{eg}} = 0$, so that the asymptotic behavior of the line shape at large ω is of a form

$$I(\omega) \sim \frac{\gamma}{\omega^2} \tag{34}$$

The asymptotic behavior, given by eq 34, has a more general meaning than being just a property of a Lorentzian distribution. It is a rather general property of a Fourier transform that is being formulated for even functions $J(t)$ with $J(0) = 0$. Note that the time domain response function, being extended to negative values of t, has the above property implying that $J(t)$ has a nonzero first time derivative at $t = 0$. In formal terms

$$\overline{J}' = \lim_{t \to +0} \frac{\mathrm{d}J(t)}{\mathrm{d}t} = -\gamma \tag{35}$$

so that, starting with analytical evaluation of the time derivative in eq 35, we can analyze the line shapes for the disorder models considered in numerical simulations. The value of γ is identified by using an asymptotic expansion

$$1 - \overline{J}(t) = p_j \int \mathrm{d}\boldsymbol{r}\, \rho(\boldsymbol{r}) \int \mathrm{d}\boldsymbol{n} \sum_j \int \mathrm{d}\boldsymbol{r}_j\, \rho_j(\boldsymbol{r}_j) h(\boldsymbol{r}_j - \boldsymbol{r}, \boldsymbol{n}, t) + O(t^2) = \gamma t + O(t^2) \tag{36}$$

for $t \to +0$.

For the $\alpha = 1$ case of complete disorder we have $\rho_j(\boldsymbol{r}_j) = {a_0}^{-3}$ and $\rho(\boldsymbol{r}) = {a_0}^{-3}$, when $\boldsymbol{r}_j$ and $\boldsymbol{r}$ belong to their cells of residence, and 0 otherwise. We can then recast eq 36 in a more convenient form

$$\frac{p_j}{{a_0}^6} \int \mathrm{d}\boldsymbol{r} \int \mathrm{d}\boldsymbol{n} \int \mathrm{d}\mathbf{x}\, h(\mathbf{x} - \boldsymbol{r}, \boldsymbol{n}, t) = \gamma t + O(t^2) \tag{37}$$

where integration over $\boldsymbol{r}$ and $\boldsymbol{x}$ goes over the chromophore cell and all TLS cells, respectively.

However, as we will see, the expansion of the right-hand side (rhs) of eq 37 does not have a form of the aforementioned equation, with the leading term being $\sim t^\beta$ with a fractional value of β. Therefore we introduce the line shape function $g(t)$, so that

$$\overline{J}(t) = \mathrm{e}^{-g(t)} \tag{38}$$

and study its short- and long-time asymptotic behavior, starting with the latter. To that end we represent

$$\ln \overline{J}(t, \boldsymbol{r}, \boldsymbol{n}) = \sum_j \ln\left(1 - \frac{p_j}{{a_0}^3} \int_{\mathcal{U}_j} \mathrm{d}\boldsymbol{r}_j\, h(\boldsymbol{r}_j - \boldsymbol{r}, t)\right) = \sum_j \ln \overline{J}_j(t, \boldsymbol{r}, \boldsymbol{n}) \tag{39}$$

where $\mathcal{U}_j$ is the residence cell of the jth TLS. We further note that for $|\boldsymbol{r}_j| \gg a_0$ and $\Omega(\boldsymbol{r}_j t) \lesssim 1$, the $h(\boldsymbol{r}_j - \boldsymbol{r}, t)$ does not change much within the cell $\mathcal{U}_j$, as a function of $\boldsymbol{r}_j$ as well as $\boldsymbol{r}$. Thus, we can first set $\boldsymbol{r} = 0$ and further replace in the rhs of eq 39

$$\ln \overline{J}_j(t, \boldsymbol{r}, \boldsymbol{n}) = \frac{1}{{a_0}^3} \int_{\mathcal{U}_j} \mathrm{d}\boldsymbol{r}_j \ln(1 - p_j h(\boldsymbol{r}_j, t)) \tag{40}$$

We can also make the same replacement given by eq 40 for those cells which correspond to $\Omega(\boldsymbol{r}_j)t \ll 1$ or $\Omega(\boldsymbol{r}_j)t \gg 1$, as it is possible to approximate $h(\boldsymbol{r}_j, t) = 1$ and $h(\boldsymbol{r}_j, t) = 0$, respectively, for the two cases. Since in the case $Bt/{a_0}^3 \gg 1$ any cell falls into at least one of the three categories described above, we obtain

$$\ln \overline{J}(t, \boldsymbol{r}, \boldsymbol{n}) = -\sum_j \int_{\mathcal{U}_j} \mathrm{d}\boldsymbol{r}_j \ln(1 - p_j h(\boldsymbol{r}_j, t)) = -\int_{\mathcal{U}} \mathrm{d}\boldsymbol{r} \ln(1 - p_j h(\boldsymbol{r}, t)) \tag{41}$$

where $\mathcal{U} = \cup_j \mathcal{U}_j$ is the region occupied by all TLSs' residence cells. Since the integral in the rhs of eq 41 converges at large r, and since each cell provides a small contribution to $g(t)$, we can extend this integration from $\mathcal{U} \subset \mathbb{R}^3$ to the whole Euclidian space $\mathbb{R}^3$, which results in the following expression for the line shape function:

$$g(t) = -\int \mathrm{d}\boldsymbol{r} \ln(1 - p_j h(\boldsymbol{r}, t)) \tag{42}$$

Note that strictly speaking the presented derivation identifies the rhs of eq 42 with $-\ln \overline{J}(t, \boldsymbol{r}, \boldsymbol{n})$, rather than with the line shape function $g(t)$. However, the rhs of eq 42 obviously turns out to be independent of $\boldsymbol{r}$ and $\boldsymbol{n}$, i.e., $\ln \overline{J}(t, \boldsymbol{r}, \boldsymbol{n}) = \ln \overline{J}(t)$, so that averaging of $\overline{J}(t, \boldsymbol{r}, \boldsymbol{n})$ with respect to $\boldsymbol{r}$ and $\boldsymbol{n}$ does not lead to any changes. Thus, we can identify $g(t) = -\ln \overline{J}(t)$, which results in eq 42.

The integral in eq 42 can be calculated explicitly in exactly the same manner in which the integral in eq 27 has been evaluated, i.e., by switching to the variables $(x, \hat{\mathbf{r}})$ which results in the asymptotic behavior of the line shape function which is linear in time

$$g(t) = \gamma t, \qquad \gamma = \zeta_{\mathrm{L}} \frac{B}{{a_0}^3} \tag{43}$$

dx.doi.org/10.1021/jp4080042 | J. Phys. Chem. A XXXX, XXX, XXX−XXX

with

$$\zeta_L = -\frac{4\pi}{3}\int_0^1 d\tau\ \sqrt{1+3\tau^2}\int_0^\infty dx\ \ln\left(1 - p_j + p_j x \sin\frac{1}{x}\right) \tag{44}$$

To compute the short-time asymptotic that corresponds to $Bt/a_0^3 \ll 1$, we note that in this case the contribution to $J(t)$ is dominated by configurations with $|\boldsymbol{r}_j - \boldsymbol{r}|^3/Bt \lesssim 1$, i.e., $|\boldsymbol{r}_j - \boldsymbol{r}| \ll a_0$. It is possible to obey this criterion only when both $\boldsymbol{r}_j$ and $\boldsymbol{r}$ are located in the close vicinity of the chromophore cell border, which consists of six faces. The major contribution thus comes from the coupling between the chromophore and the TLS that reside in the unit cells sharing a common face. Integration over $\boldsymbol{r}$ and $\boldsymbol{r}_j$, which is restricted to the region described above, can be performed using the following variables: $r = |\boldsymbol{r}_j - \boldsymbol{r}|$, $\boldsymbol{\eta} = \hat{\mathbf{r}}_j$, the position $\boldsymbol{z}$ where the segment connecting $\boldsymbol{r}$ to $\boldsymbol{r}_j$ crosses the face, and $s \in [0,1] = |\boldsymbol{r}_j - \boldsymbol{z}|/r$, so that we have

$$\boldsymbol{r}_j = \boldsymbol{z} + s\boldsymbol{\eta}, \qquad \boldsymbol{r} = \boldsymbol{z} - (1-s)\boldsymbol{\eta} \tag{45}$$

Integration over $\boldsymbol{z}$ goes over the chromophore cell border, represented by 6 faces, and in the case of short times we can extend integrations over r, s, and $\boldsymbol{\eta}$ to $(0, \infty)$, $[0, 1]$, and a hemisphere, respectively. This yields

$$1 - \overline{J}(t) = \frac{p_j}{a_0^6}\int d\boldsymbol{z}\int_{S^2_-} 4\pi(\boldsymbol{\tau}\cdot\boldsymbol{\eta})\, d\boldsymbol{\eta}\int_{S^2} d\boldsymbol{n}\int_0^1 ds \int_0^\infty r^3 dr\left(1 - \frac{\sin(Bt\sqrt{1+3(\boldsymbol{\eta}\cdot\boldsymbol{n})^2}\, r^{-3})}{Bt\sqrt{1+3(\boldsymbol{\eta}\cdot\boldsymbol{n})^2}\, r^{-3}}\right) \tag{46}$$

where S^2 and S^2_- denote the unit sphere and hemisphere, respectively, and $\boldsymbol{\tau}$ denotes the normal vector to the surface of the border. The additional factors in eq 46 are due to the integration measure, written in new variables, i.e., $d\boldsymbol{r}\, d\boldsymbol{r}_j = 4\pi(\boldsymbol{\tau}\cdot\boldsymbol{\eta})\, d\boldsymbol{z}\, r^3 dr\, d\boldsymbol{\eta}$.

Integration in eq 46 can be performed explicitly. We first integrate over r, switching to the variable x, introduced earlier. We then integrate over $\boldsymbol{n}$, which eliminates the dependence on $\boldsymbol{\eta}$, so that the integrals over $\boldsymbol{\eta}$ and $\boldsymbol{z}$ in eq 46 are factorized, and we compute

$$\int_{S^2_-} 4\pi(\boldsymbol{\tau}\cdot\boldsymbol{\eta})\, d\boldsymbol{\eta} = \int_0^{2\pi} d\varphi\int_0^{\pi/2} d\theta\, \sin\theta\cos\theta = \pi \tag{47}$$

as well as

$$\int_{\partial\mathcal{U}_0} d\boldsymbol{z} = 6a_0^2 \tag{48}$$

This results in

$$\overline{J}(t) \sim 1 - \zeta_s(\gamma_0 t)^{4/3} \tag{49}$$

and

$$\zeta_s = 4\pi p_j\int_0^1 d\tau\ (1+3\tau^2)^{2/3}\int_0^\infty dx\ x^{1/3}\left(1 - x\sin\left(\frac{1}{x}\right)\right) \tag{50}$$

To summarize, we identified the short- and long-time asymptotic behavior of the line shape function for our $\alpha = 1$ model of disorder as

$$g(t) = \zeta_s(\gamma_0 t)^{4/3}, \quad \text{for } \gamma_0 t \ll 1$$
$$g(t) = \zeta_L(\gamma_0 t), \quad \text{for } \gamma_0 t \gg 1 \tag{51}$$

We next proceed to compare the analytically predicted time-domain response function with that obtained from the numerical simulations with $\alpha = 1.0$. Numerical evaluation of eq 50 yields a value of $\zeta_s = 6.36$ corresponding to the short-time asymptotic limit. Using this value, as shown clearly in Figure 7,

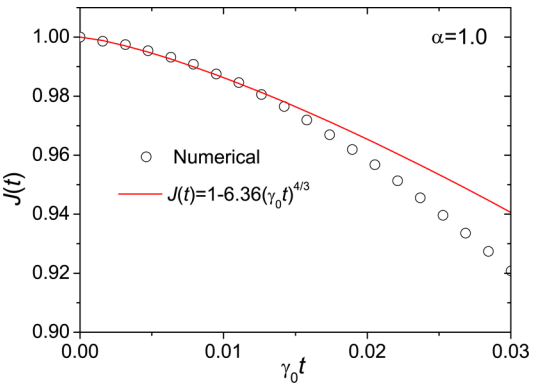

Figure 7. For completely disordered environment ($\alpha = 1.0$), averaged response function calculated from numerical simulations (hollow circles) and its comparison with the analytical expressions of eqs 49 and 50 in the short-time limit.

a satisfactory fitting of the numerical data by eq 49 is obtained. In the long-time limit, on the other hand, the calculated value of $\zeta_L = 2.853$ from eq 44 is found to be nearly 2 times smaller than that obtained as 5.23 by fitting $\overline{J}(t)$. This discrepancy can be attributed to subtle differences between the models of disorder considered in the analytical and the numerical treatments, considering that the latter involves chromophore at a substitutional site. To seek an improved agreement, we consider a slightly modified model for the numerical simulations in which an additional TLS is allowed to share the cubic unit cell of the central chromophore. The chromophore is fixed at the center, while its dipole directions are assigned randomly. All the remaining 1331 TLSs are completely disordered ($\alpha = 1.0$). Under these constraints, the Lorentzian profile of the resulting line shape is found to have a reduced fwhm. Fitting the corresponding $\overline{J}(t)$ with an exponential function yields a value of $\zeta_L = 2.79$, which is in much better agreement with the analytical predictions.

D. Homogeneous Disorder Model. We complete our analysis via studying another model of disorder that allows for an analytical solution and provides a family of line shape functions depending on the value of a control parameter, admitting the Gaussian and Lorentzian forms in the extreme cases. Such models are based on independent distribution of identical noninteracting TLSs with the distribution function $\rho(\boldsymbol{r})$ being not completely homogeneous, but rather spherically symmetric with respect to the chromophore position, unfavoring the TLS to come too close to the chromophore. For the sake of simplicity we consider a hard-core sphere model, when $\rho(r) = 0$ for $|r| < r_0$, and is constant otherwise, so that r_0 plays the role of a parameter. In the thermodynamic limit the line shape function adopts a form

dx.doi.org/10.1021/jp4080042 | J. Phys. Chem. A XXXX, XXX, XXX−XXX

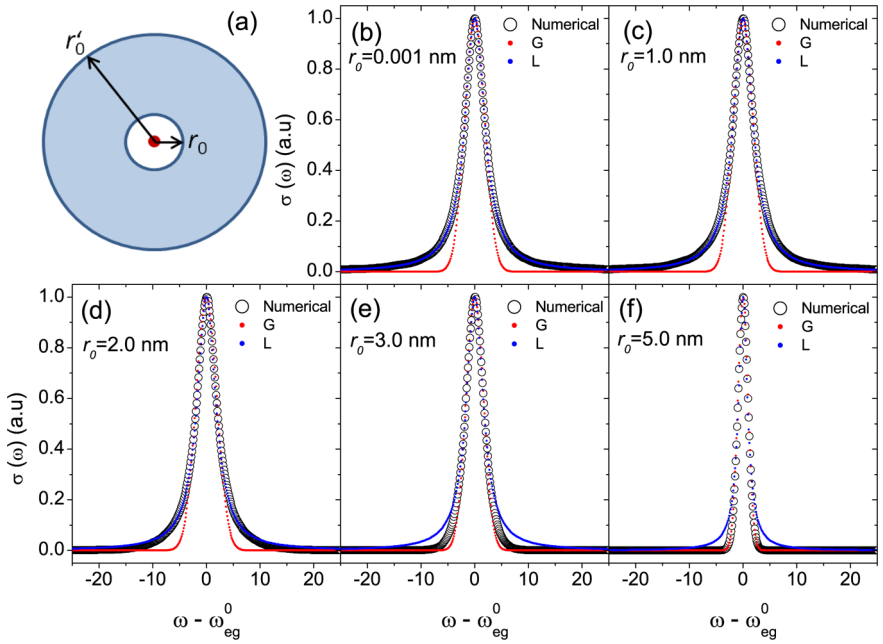

Figure 8. (a) Schematic of a model in which the TLSs are uniformly distributed in a spherical shell (highlighted) centered on the single chromophore (red dot). (b–f) Calculated absorption line shape (hollow circles, black) for this model with r_0 = 0.001, 1.0, 2.0, 3.0, and 5.0 nm, respectively. Corresponding fits by a Gaussian function (G, in red points) and a Lorentzian function (L, in blue points) are also shown.

$$g(t) = 4\pi p_j a_0^{-3} \int_{S^2} d\hat{\boldsymbol{r}} \int_{r_0}^{\infty} r^2 \, dr \left(1 - \frac{\sin(Bt\sqrt{1 + 3(\hat{\boldsymbol{r}}\cdot\boldsymbol{n})^2 r^{-3}})}{Bt\sqrt{1 + 3(\hat{\boldsymbol{r}}\cdot\boldsymbol{n})^2 r^{-3}}}\right) \tag{52}$$

with $a_0 = n^{-1/3}$, n being the TLS concentration. Introducing the function

$$F(x) = \int_x^{\infty} dy \left(1 - y \sin\left(\frac{1}{y}\right)\right) \tag{53}$$

and invoking the variable transformation we have used several times throughout this paper, we arrive at

$$g(t) = \frac{4\pi}{3}\gamma_0 t \int_0^1 d\tau \sqrt{1 + 3\tau^2} F(x_0(t, \tau; r_0))$$

$$x_0(t, \tau; r_0) = \frac{r_0^3}{Bt\sqrt{1 + 3\tau^2}} \tag{54}$$

In the case of $r_0 \ll a_0$, we can set $r_0 = 0$ in eq 54, and naturally reproduce eq 32 upon using $F(0) = \pi/4$. In the opposite case $r_0 \gg a_0$, for relevant values of t we have $x_0(t, \tau; r_0) \gg 1$, and we can use the asymptotic form $F(x_0) \sim 1/(6x_0)$, which results in the Gaussian shape of the line shape function

$$g(t) = \frac{\sigma t^2}{2}, \qquad \sigma = \frac{4\pi}{9}\gamma_0^2 \tag{55}$$

In the crossover region the line shape function $g(t)$ looks pretty complicated, as one can see from eq 54.

Finally, we carry out numerical simulations based on this generic hard-core model of disorder in TLSs. As shown in the schematic of Figure 8a, the chromophore with randomly oriented dipole is fixed to the origin and 1331 TLSs are uniformly distributed inside a spherical shell around it. The inner radius of the shell (r_0) serves as the control parameter, and the outer radius (r_0') can be chosen so as to yield a density identical to that used in the lattice-based model. With an increase in r_0, the smallest possible separation between the chromophore and the TLSs increases, thereby influencing the line shape. From Figure 8b, it can be easily observed that the calculated absorption line shape for the case of negligible separation, r_0 = 0.001 nm, is perfectly Lorentzian. Even with a small clearance allowed in the cases of r_0 = 1.0 nm and r_0 = 2.0 nm, which carries more appropriate physical meaning owing to the finite size of the TLSs and the chromophore, the Lorentzian profile is preserved well as is evident from Figure 8c,d. As r_0 is increased further, deviations from the Lorentzian profile start to appear. In particular, in the intermediate regime, represented by r_0 = 3.0 nm, the calculated line shape is neither Lorentzian nor Gaussian and assumes a complicated profile. More interestingly, when the minimum distance between chromophore and TLSs becomes large enough, as in Figure 8f with r_0 = 5.0 nm, one can note that the line shape pertains well to a Gaussian curve. The numerical results obtained here are thus in perfect agreement with the analytical predictions of the line shapes in both limiting cases.

E. Further Discussions. In this work, especially for carrying out the numerical simulations, we have employed the necessary parameters which have been derived for terrylene in polystyrene; however, they are regarded in general to be representative of typical glassy matrixes. We also note that the experimentally measured values of the line widths are on the order of gigahertz, for example, for terrylene in polystyrene.[3] The fwhm of the spectral lines calculated in this work can, however, be as large as 30 GHz for the case of α = 1.0 (cf. Figure 3d) in the lattice-based model. The TLS specific parameters (A_j and M_j) employed in this work yield a TLS energy splitting (ϵ_j/k_B) of 0.01 K, which is much smaller than the system temperature T = 1.7 K. This results in the probability of a TLS being in the excited state equal to 0.5, implying the high-temperature regime with respect to thermal occupation of TLSs. The average energy splitting of the TLSs

dx.doi.org/10.1021/jp4080042 | J. Phys. Chem. A XXXX, XXX, XXX–XXX

surrounding a given chromophore in experimental systems can, however, be on the order of a few kelvin as estimated in earlier studies.[36] This implies that in our simulations, considering the parameter regime employed, a greater number of "active" TLSs are dispersed surrounding the chromophore as compared to the chromophores studied in experiments, which leads to stronger modulation of the chromophore's frequency and thus to greater line widths. We have carried out additional calculations by employing the lattice-based model for two different sets of TLS parameters $[(A_j,J_j) = (0.6\text{ K}, 0.8\text{ K})$ and $(3.0\text{ K}, 4.0\text{ K})]$, while keeping all the other parameters identical to those used in this work. The corresponding energy splitting of the TLSs is then 1 and 5 K, respectively. As shown in Figure 9a,b, the calculated

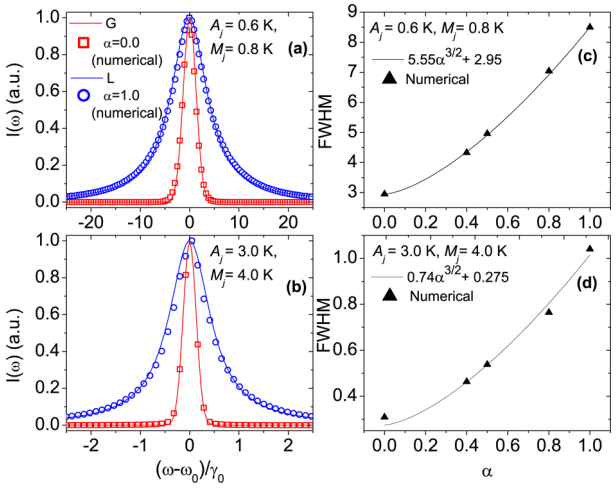

Figure 9. Calculated absorption line shapes for α = 0.0 (hollow squares, red) and α = 1.0 (hollow circles, blue) for (a) A_j = 0.6 K and M_j = 0.8 K, and (b) A_j = 3.0 K and M_j = 4.0 K. Corresponding fitting with the Gaussian curve (G) for α = 0.0 and with the Lorentzian (L) for α = 1.0 are shown as unbroken curves. (c, d) fwhm of the absorption peaks as a function of α shown for the same set of parameters within each horizontal panel.

line shapes for both cases are found to be fitted well by a Gaussian curve when α = 0 and by a Lorentzian curve when α = 1.0, thereby establishing the robustness of our results on the effect of disorder on the absorption line shapes. The power-law dependence of the fwhm on α described earlier can also seen to be followed reasonably well in Figure 9c,d. For ϵ_j/k_B = 1 K, one obtains a slight reduction in p_j to 0.36 and, accordingly, the fwhm is found to be reduced to 21.99 GHz for α = 1.0. With an even higher ϵ_j/k_B = 5 K, p_j = 0.05, which leads to the line width of 2.7 GHz, that compares reasonably well with the peak of the measured line-width distribution.[3,42] In a similar manner, agreement with the experimental observations is also achieved for the homogeneous disorder (hard-core) model studied in this subsection when a minimum chromophore−TLS separation is set to 5 nm, similar to the estimated separation in other studies.[42,44] Our results for this case show the average fwhm reduced to nearly 5.7 GHz (cf. Figure 8f), which is within the experimentally reported range.

IV. CONCLUSIONS

Spectroscopic studies of single molecules provide a unique opportunity for probing the submicroscopic structure and dynamics of their environment, especially for disordered materials. Absorption line shapes measured for different chromophore−host systems have revealed a rather wide array of spectral characteristics that have been analyzed by theoretical studies to validate the standard tunneling TLS model for glasses. Modeling the host matrix as TLSs occupying regular lattice positions, Orth et al. found the line shape of the chromophore to change from Lorentzian to Gaussian forms as the defect density is varied from its smallest to its largest values.[41] Based on a similar model of TLS distribution and using the stochastic sudden jump model, Reilly and Skinner calculated the line shape over a wide range of parameter space.[35] It was revealed that a Lorentzian line shape arises when the probability of the TLSs to be in an excited state is very small. Brown and Silbey demonstrated that the influence of TLS−TLS coupling on the chromophore's line shape is negligible.[44] In general, however, the existing literature reports have been dominated by the investigation of time-domain features such as spectral diffusion as compared to the frequency-domain line shape studies. In this paper, we have carried out a systematic study of absorption line shape of a chromophore embedded in a typically disordered solid environment such as glasses. By modeling the chromophore as an electronic TLS and the host matrix as a collection of tunneling TLSs, we have analytically as well as numerically probed the influence of spatial and steric disorder of the matrix within the stochastic sudden jump model. Numerical simulations on the lattice-based model in which the chromophore and the TLSs are located on points on a simple cubic lattice, i.e., in the absence of disorder, reveal the absorption line shape to be of inhomogeneously broadened Gaussian form. In a completely disordered or glassy environment, however, it is found to be of homogeneously broadened Lorentzian profile. Further simulations in which a certain minimum chromophore−TLS separation is imposed by constraining the chromophore and its nearest-neighbor TLSs to occupy the lattice sites were found to yield a Gaussian profile despite complete disorder of the remaining TLSs. The Lorentzian line shape of the chromophore in glassy media is thus found to originate from the strongly enhanced coupling between the chromophore and a TLS in close proximity. The numerical simulations thus provide crucial insights in uncovering the dominant effects of close chromophore−TLS pairs in causing non-Gaussian deviations in the absorption line shape.

To rationalize the dependence of the line shape on the disorder in TLSs, we have also carried out a detailed theoretical study. We prove that as a long as the criterion of sufficiently large chromophore−TLS separation is obeyed, under the condition of fixed position and dipole direction of the chromophore, the resulting line shape should be a Gaussian function irrespective of the spatial and steric disorder in the TLSs. Furthermore, we have developed a theoretical framework to describe the origin of the Lorentzian line shape in the case of complete disorder based on an equivalent model. The analytical predictions in both extreme cases, i.e., α = 0 and α = 1, on the time-domain reponse function have been shown to be supported well by the numerical results. For the sake of completeness, we have also studied a much more generic model of disorder in which the chromophore fixed at the origin is surrounded by the TLSs distributed uniformly within a concentric spherical shell. By modulating the control parameter, which is the inner diameter of the shell r_0, it is shown to lead to both limiting cases, i.e., the Gaussian line shape in the limit of

dx.doi.org/10.1021/jp4080042 | J. Phys. Chem. A XXXX, XXX, XXX−XXX

large r_0 and the Lorentzian line shape in the opposite limit of vanishing r_0.

The present work is focused on the investigation of the influence of positional disorder of TLSs on the spectral characteristics of an embedded chromophore. In a realistic system, according to the standard tunneling TLS model, the characteristic parameters of the TLSs are assumed to follow certain distributions. We have adopted the assumption of identical TLSs in order to simplify the analysis and have chosen the TLS parameters suitably to correspond to the high-temperature regime. The parameter regime thus specified allows us to derive a simple expression for the time-domain response function and, subsequently, the line shape for the chromophore embedded in static TLSs in a high-temperature regime. The relatively small energy splitting of the TLSs as compared to the system temperature for the parameter regime in our work implies that, in realistic systems, where TLS flipping may be associated with the motion of domain walls,[36,42] such TLSs are likely to be situated very close to a domain boundary. Accordingly, the comparison of our results on spectral line shapes with experimental results can be seen to be most relevant for the line shapes measured for individual chromophores which interact with the TLSs situated near domain walls. In the early studies, it has been found that, for the TLSs distributed on a regular lattice, the absorption line shape is Gaussian in the high-temperature limit, i.e., when the probability of a given TLS to be in an excited state is 0.5. We have demonstrated under the same condition that when spatial and steric disorder effects are taken into account, which are more likely to mimic the realistic distribution, the line shape may even morph into a Lorentzian profile. Furthermore, our results based on both the lattice-based model and the homogenously distributed model show that the line shape observed remains Gaussian irrespective of the degree of disorder of the relatively distant TLSs, provided that the minimum TLS−chromophore separation is sufficiently large enough. The Lorentzian line shape is realized due to the strong modulation in the chromophore's frequency by closely spaced TLSs.

Finally, we draw an interesting parallel of our current findings to the important role played by static disorder on magnetic hysteresis in finite sized single-domain micromagnetic particle arrays.[56,57] In two-dimensional arrays, it was found that an increase in the disorder leads to an increase in the coercivity.[56] Similar results were also demonstrated earlier for three-dimensional systems apart from the fact that in this case there exists no hysteresis without disorder.[57] Our current work may thus help emphasize the importance of disorder in the immediate microscopic environment, in governing the macroscopic properties of a system of interest.

AUTHOR INFORMATION

Corresponding Author

*E-mail: YZhao@ntu.edu.sg. Tel.: +(65) 65137990.

Notes

The authors declare no competing financial interest.

ACKNOWLEDGMENTS

Support by the Singapore National Research Foundation through the Competitive Research Programme (CRP) under Project No. NRF-CRP5-2009-04 is gratefully acknowledged. This work is also supported in part by the U.S. National Science Foundation under Grant CHE-1111350.

REFERENCES

(1) Barkai, E.; Jung, Y. J.; Silbey, R. Theory of Single-Molecule Spectroscopy: Beyond the Ensemble Average. *Annu. Rev. Phys. Chem.* **2004**, *55*, 457−507.

(2) Tamarat, Ph.; Lounis, M. B.; Orrit, M. Ten Years of Single-Molecule Spectroscopy. *J. Phys. Chem. A* **2000**, *104*, 1−16.

(3) Kozankiewicz, B.; Bernard, J.; Orrit, M. Single Molecule Lines and Spectral Hole Burning of Terrylene in Different Matrices. *J. Chem. Phys.* **1994**, *101*, 9377−9383.

(4) Orrit, M.; Bernard, J. Single Pentacene Molecules Detected By Fluorescence Excitation in a p-Terphenyl Crystal. *Phys. Rev. Lett.* **1990**, *65*, 2716−2719.

(5) Zumbrusch, A.; Fleury, L.; Brown, R.; Bernard, J.; Orrit, M. Probing Individual Two-Level Systems in a Polymer by Correlation of Single Molecule Fluorescence. *Phys. Rev. Lett.* **1993**, *70*, 3584−3587.

(6) Schmidt, T.; Baak, J.; van de Straat, D. A.; Brom, H. B.; Völker, S. Temperature Dependence of Optical Linewidths and Specific Heat of Rare-Earth-Doped Silicate Glasses. *Phys. Rev. Lett.* **1993**, *71*, 3031−3034.

(7) Fleury, L.; Zumbrusch, A.; Brown, R.; Bernard, J. Spectral Diffusion and Individual Two-level Systems Probed by Fluorescence of Single Terrylene Molecules in a Polyethylene Matrix. *J. Lumin.* **1993**, *56*, 15−28.

(8) Kettner, R.; Tittel, J.; Basché, T.; Bräuchle, C. Optical Spectroscopy and Spectral Diffusion of Single Dye Molecules in Amorphous Spin-Coated Polymer Films. *J. Phys. Chem.* **1994**, *98*, 6671−6674.

(9) Tittel, J.; Kettner, R.; Basché, T.; Bräuchle, C.; Quante, H.; Müllen, K. Spectral Diffusion in an Amorphous Polymer Probed by Single Molecule Spectroscopy. *J. Lumin.* **1995**, *64*, 1−11.

(10) Kozankiewicz, B.; Bernard, J.; Orrit, M. Single Molecule Lines and Spectral Hole Burning of Terrylene in Different Matrices. *J. Chem. Phys.* **1994**, *101*, 9377−9383.

(11) Sevian, H. M.; Skinner, J. L. Molecular Theory of Transition Energy Correlations for Pairs of Chromophores in Liquids or Glasses. *J. Chem. Phys.* **1992**, *97*, 8−18.

(12) Stoneham, A. M. Shapes of Inhomogeneously Broadened Resonance Lines in Solids. *Rev. Mod. Phys.* **1969**, *41*, 82−108.

(13) Messing, I.; Raz, B.; Jortner, J. Medium Perturbations of Atomic Extravalence Excitations. *J. Chem. Phys.* **1977**, *66*, 2239−2251.

(14) Messing, I.; Raz, B.; Jortner, J. Solvent Perturbations of Extravalence Excitations of Atomic Xe by Rare Gases at High Pressures. *J. Chem. Phys.* **1977**, *66*, 4577−4586.

(15) Phillips, W. A. Two-level States in Glasses. *Rep. Prog. Phys.* **1987**, *50*, 1657−1708.

(16) Anderson, P. W.; Halperin, B. I.; Varma, C. M. Anomalous Low-temperature Thermal Properties of Glasses and Spin-glasses. *Philos. Mag.* **1972**, *25*, 1−9.

(17) Phillips, W. A. Tunneling States in Amorphous Solids. *J. Low Temp. Phys.* **1972**, *3/4*, 351−360.

(18) Zeller, R. C.; Pohl, R. O. Thermal Conductivity and Specific Heat of Noncrystalline Solids. *Phys. Rev. B* **1971**, *4*, 2029−2041.

(19) Black, J. L.; Halperin, B. I. Spectral Diffusion, Phonon Echoes, and Saturation Recovery in Glasses at Low Temperatures. *Phys. Rev. B* **1977**, *16*, 2879−2895.

(20) Jankowiak, R.; Small, G. J. Thermal Conductivity in Amorphous Solids at Temperatures Below 1 K. *Phys. Rev. B* **1987**, *37*, 8407−8411.

(21) Jankowiak, R.; Hayes, J. M.; Small, G. J. Low-Temperature Sspecific Heat of Glasses: Temperature and Time Dependence. *Phys. Rev. B* **1988**, *38*, 2084−2088.

(22) Golding, B.; Graebner, J. E.; Halperin, B. I.; Schutz, R. J. Nonlinear Phonon Propagation in Fused Silica below 1 K. *Phys. Rev. Lett.* **1973**, *30*, 223−226.

(23) Golding, B.; Graebner, J. E. Phonon Echoes in Glass. *Phys. Rev. Lett.* **1976**, *37*, 852−855.

(24) Heuer, A.; Silbey, R. J. Tunneling in Real Structural Glasses: A Universal Theory. *Phys. Rev. B* **1994**, *49*, 1441−1444.
(25) Heuer, A.; Silbey, R. J. Microscopic Estimation of the Deformation Potential in a Structural Model Glass. *Phys. Rev. B* **1993**, *48*, 9411−9417.
(26) Narasimhan, L. R.; Littau, K. A.; Pack, D. W.; Bai, Y. S.; Elschner, A.; Fayer, M. D. Probing Organic Glasses at Low Temperature with Variable Time Scale Optical Dephasing Measurements. *Chem. Rev.* **1990**, *90*, 439−457.
(27) Berret, J. F.; Meissner, M. Z. How Universal Are The Low Temperature Acoustic Properties of Glasses? *Phys. B (Amsterdam, Neth.)* **1988**, *70*, 65−72.
(28) Heuer, A.; Silbey, R. Microscopic Description of Tunneling Systems in a Structural Model Glass. *Phys. Rev. Lett.* **1993**, *70*, 3911−3914.
(29) Dab, D.; Heuer, A.; Silbey, R. J. Low Temperature Properties of Glasses: A Preliminary Study of Double Well Potentials Microscopic Structure. *J. Lumin.* **1995**, *64*, 95−100.
(30) Lubchenko, V.; Wolynes, P. G. Intrinsic Quantum Excitations of Low Temperature Glasses. *Phys. Rev. Lett.* **2001**, *87*, 195901/1−195901/4.
(31) Boiron, A. M.; Tamarat, P.; Lounis, B.; Brown, R.; Orrit, M. Are the Spectral Trails of Single Molecules Consistent With the Standard Two-Level System Model of Glasses at Low Temperatures? *Chem. Phys.* **1999**, *247*, 119−132.
(32) Klauder, J. R.; Anderson, P. W. Spectral Diffusion Decay in Spin Resonance Experiments. *Phys. Rev.* **1962**, *125*, 912−932.
(33) Huber, D. L. Analysis of a Stochastic Model for the Optical and Photon-Echo Decays of Impurities in Glasses. *J. Lumin.* **1987**, *36*, 307−314.
(34) Reilly, P. D.; Skinner, J. L. Spectral Diffusion of Single Molecule Fluorescence: A Probe of Low-Frequency Localized Excitations in Disordered Crystals. *Phys. Rev. Lett.* **1993**, *71*, 4257−4260.
(35) Reilly, P. D.; Skinner, J. L. Spectroscopy of a Chromophore Coupled to a Lattice of Dynamic Two-level Systems. I. Absorption Line Shape. *J. Chem. Phys.* **1994**, *101*, 959−963.
(36) Reilly, P. D.; Skinner, J. L. Spectral Diffusion of Individual Pentacene Molecules in p-Terphenyl Crystal: Stochastic Theoretical Model and Analysis of Experimental Data. *J. Chem. Phys.* **1995**, *102*, 1540−1552.
(37) Geva, E.; Skinner, J. L. Optical Line Shapes of Single Molecules in Glasses: Temperature and Scan-Time Dependence. *J. Chem. Phys.* **1998**, *109*, 4920−4926.
(38) Zhao, Y.; Chernyak, V.; Mukamel, S. Spin Versus Boson Baths in Nonlinear Spectroscopy. *J. Phys. Chem. A* **1998**, *102*, 6614−6634.
(39) Suarez, A.; Silbey, R. Study of a Microscopic Model for Two-Level System Dynamics in Glasses. *J. Phys. Chem.* **1994**, *98*, 7329−7336.
(40) Zumofen, G.; Klafter, J. Spectral Random Walk of a Single Molecule. *Chem. Phys. Lett.* **1994**, *219*, 303−309.
(41) Orth, D. L.; Mashl, R. J.; Skinner, J. L. Optical Lineshapes of Impurities in Crystals: A Lattice Model of Inhomogeneous Broadening by Point Defects. *J. Phys.: Condens. Matter* **1993**, *5*, 2533−2544.
(42) Geva, E.; Reilly, P. D.; Skinner, J. L. Spectral Dynamics of Individual Molecules in Glasses and Crystals. *Acc. Chem. Res.* **1996**, *29*, 579−584.
(43) Geva, E.; Skinner, J. L. Theory of Single-Molecule Optical Line-Shape Distributions in Low-Temperature Glasses. *J. Phys. Chem. B* **1997**, *101*, 8920−8932.
(44) Brown, F. L. H.; Silbey, R. J. An Investigation of the Effects of Two Level System Coupling on Single Molecule Lineshapes in Low Temperature Glasses. *J. Chem. Phys.* **1998**, *108*, 7434−7450.
(45) Naumov, A. V.; Vainer, Yu. G.; Bauer, M.; Kador, L. Moments of Single-Molecule Spectra in Low-Temperature Glasses: Measurements and Model Calculations. *J. Chem. Phys.* **2002**, *116*, 8132−8138.
(46) Wu, N.; Zhao, Y. Dynamics of a Two-Level System Under the Simultaneous Influence of a Spin Bath and a Boson Bath. *J. Chem. Phys.* **2013**, *139*, 054118/1−054118/11.
(47) Mims, W. B.; Nassau, K.; McGee, J. D. Spectral Diffusion in Electron Resonance Lines. *Phys. Rev.* **1961**, *123*, 2059−2069.
(48) Mims, W. B. Phase Memory in Electron Spin Echoes, Lattice Relaxation Effects in CaWO4: Er, Ce, Mn. *Phys. Rev.* **1968**, *168*, 370−389.
(49) Maynard, R.; Rammal, R.; Suchail, R. Spectral Diffusion Decay of Spontaneous Echoes in Disordered Systems. *J. Phys., Lett.* **1980**, *41*, 291−294.
(50) Kassner, K.; Silbey, R. Interactions of Two-Level Systems in Glasses. *J. Phys.: Condens. Matter* **1989**, *1*, 4599−4610.
(51) Joffrin, J.; Levelut, A. Virtual Phonon Exchange in Glasses. *J. Phys. (Paris)* **1975**, *36*, 811−822.
(52) Grannan, E. R.; Randeria, M.; Sethna, J. P. Low-Temperature Properties of a Model Glass. I. Elastic dipole model. *Phys. Rev. B* **1990**, *41*, 7784−7798.
(53) Slichter, C. P. *Principles of Magnetic Resonance*; Springer-Verlag: Berlin, Germany, 1990.
(54) Meltzer, R. S.; Yen, W. M.; Zheng, H.; Feofilov, S. P.; Dejneka, M. J.; Tissue, B. M.; Yuan, H. B. Evidence for Long-Range Interactions Between Rare-Earth Impurity Ions in Nanocrystals Embedded in Amorphous Matrices With the Two-Level Systems of the Matrix. *Phys. Rev. B* **2001**, *64*, 100201(R)/1−100201(R)/4.
(55) Bell, G.; Zheng, Y. J.; Brown, F. L. H. Single Molecule Photon Counting Statistics for Quantum Mechanical Chromophore Dynamics. *J. Phys. Chem. B* **2006**, *110*, 19066−19082.
(56) Yang, B.; Zhao, Y. Coercivity Control in Finite Arrays of Magnetic Particles. *J. Appl. Phys.* **2011**, *110*, 103908/1−103908/7.
(57) Zhao, Y.; Bertram, H. N. Disorder and Coercivity in Magnetic Particle Systems. *J. Magn. Magn. Mater.* **1992**, *114*, 329−335.